Dispersion of Time Domain Wavelet Galerkin Method Based on Daubechies' Compactly Supported Scaling Functions with Three and Four Vanishing Moments

Masafumi Fujii and Wolfgang J. R. Hoefer

***Abstract*—The wavelet-Galerkin method for time-domain electromagnetic field modeling based on Daubechies' compactly supported wavelets proposed by Cheong *et al.*has been extended to the use of the scaling functions with three and four vanishing wavelet moments together with the approximate shifted interpolation property. The numerical dispersion properties of the methods are precisely investigated and compared with those of other wavelet-based and finite-difference methods. It was found that Daubechies' scaling functions with larger number of vanishing moments generally give higher accuracy while maintaining the comparable computational expenditure.**

***Index Terms*—Daubechies' compactly supported wavelets, electromagnetic field analysis, time domain, wavelet-Galerkin method.**

I. INTRODUCTION

THE WAVELET-GALERKIN scheme based on Daubechies' compactly supported wavelets with two vanishing moments proposed by Cheong *et al.* [1] demonstrates, by virtue of the shifted interpolation property of Daubechies' wavelets, high versatility and simplicity when applied to time-domain electromagnetic problems with inhomogeneous media.

As a single-channel approach where only the scaling functions are used as basis functions, Cheong's scheme [1] has advantages over the previously reported wavelet-based time-domain analysis techniques such as S-MRTD [2]; the formulation is similar to Yee's FDTD scheme [3] even for inhomogeneous media; and it does not require the incorporation of the constitutive equations of Maxwell's equations. This results in a simple algorithm despite the large support and asymmetry of Daubechies' scaling functions.

However, the improvement in accuracy and efficiency through the use of Daubechies' scaling functions has not been fully clarified. Moreover, it is expected that Daubechies' wavelets with larger number of the vanishing moments yield more effective algorithms.

In this paper, the time-domain wavelet-Galerkin method based on Daubechies' compactly supported scaling functions with two, three, and four vanishing moments (denoted as D_2, D_3, and D_4, respectively) has been investigated, and the efficiency of those schemes is compared with respect to accuracy and computational expenditure.

Manuscript received December 17, 1999; revised February 17, 2000.

The authors are with the Department of Electrical and Computer Engineering University of Victoria, Victoria, B.C. V8W 3P6, Canada (e-mail: fujii@engr.uvic.ca).

Publisher Item Identifier S 1051-8207(00)04448-2.

II. FORMULATION

Maxwell's equations for the two-dimensional (2-D) TE polarization

$$-\mu \frac{\partial H_x}{\partial t} = -\frac{\partial E_y}{\partial z} \tag{1}$$

$$-\mu \frac{\partial H_z}{\partial t} = \frac{\partial E_y}{\partial x} \tag{2}$$

$$J_y + \sigma E_y + \epsilon \frac{\partial E_y}{\partial t} = \frac{\partial H_x}{\partial z} - \frac{\partial H_z}{\partial x} \tag{3}$$

are discretized on the standard Yee grid. Following the theory in [1], the field values are first expanded in Daubechies' compactly supported scaling functions ϕ [4], which approximately satisfy the shifted interpolation property [5]

$$\phi(k + M_1) = \delta_{k,0} \tag{4}$$

for k integer, where $M_1 = \int_{-\infty}^{+\infty} x\phi(x)\,dx$ is the first-order moment of the scaling function and δ the Kronecker delta function. This property yields a simple algorithm for inhomogeneous problems through the local sampling of the field values regardless of the complexity of the inhomogeneity [1].

The standard Galerkin's procedure leads to a system of updating equations similar to the S-MRTD method [2] as

$$\begin{aligned} E^{\phi}_{y,i,k,n+1/2} &= \frac{2\epsilon - \sigma\Delta t}{2\epsilon + \sigma\Delta t} E^{\phi}_{y,i,k,n-1/2} \\ &\quad + \frac{1}{2\epsilon + \sigma\Delta t}\left[\sum_{l=-L_s}^{L_s-1} a(l)\left(\frac{H^{\phi}_{x,i,k+l+1/2,n}}{\Delta z} - \frac{H^{\phi}_{z,i+l+1/2,k,n}}{\Delta x}\right) - J^{\phi}_{y,i,k,n}\right] \end{aligned} \tag{5}$$

where L_s denotes the effective support size of the basis functions, that is, the stencil size or the number of connection coefficients per side practically included in the update equations. Equations for H_x and H_z are obtained similarly. The coefficients connecting the scaling functions and their derivatives are obtained by evaluating the inner products numerically in the Fourier domain

$$\begin{aligned} a(l) &\equiv \left\langle \frac{d\phi_{j+1/2}(x)}{dx} \middle| \phi_{j-l}(x) \right\rangle \\ &= \frac{1}{\pi}\int_0^{\infty} \omega \left|\hat{\phi}(\omega)\right|^2 \sin\left[\omega\left(l + \frac{1}{2}\right)\right] d\omega \end{aligned} \tag{6}$$

TABLE I
CONNECTION COEFFICIENTS $a(l)$, THE FIRST-ORDER MOMENTS M_1 AND THE STABILITY FACTOR FOR THE TWO-DIMENSIONAL SQUARE-GRID CASES s. PARAMETERS FOR D_{10} AND BATTLE–LEMARIÉ CUBIC SPLINE SCALING FUNCTIONS ARE SHOWN FOR THE PURPOSE OF COMPARISION

l	D_2	D_3	D_4	D_{10}	B.L.
0	1.2291666667	1.2918129281	1.3110340773	1.3033236013	1.2918462114
1	-0.0937500000	-0.1371343465	-0.1560100710	-0.1636941766	-0.1560760696
2	0.0104166667	0.0287617723	0.0419957460	0.0616127747	0.0596390461
3		-0.0034701413	-0.0086543236	-0.0265749940	-0.0293098737
4		0.0000080265	0.0008308695	0.0104549954	0.0153715666
5			0.0000108999	-0.0034151723	-0.0081892221
6			-0.0000000041	0.0008675397	0.0043787661
7				-0.0001583521	-0.0023432839
8				0.0000179275	0.0012542425
9				-0.0000007829	-0.0006713627
10				-0.0000000260	0.0003593662
11				-0.0000000072	-0.0001923616
12				0.0000000014	0.0001029674
13				0.0000000001	-0.0000551164
14				0.0000000000	0.0000295027
M_1	0.6339743121	0.8174005815	1.0053923835	—	—
s	0.5303	0.4839	0.4657	0.4504	0.4508

where $\hat{\phi}$ denotes the Fourier transform of ϕ. $a(l)$ is listed in Table I together with the first-order moment M_1 and the stability factor for the 2-D square-grid case $s = 1/(\sqrt{2}\sum_l |a(l)|)$. It is interesting to note that, although ϕ is not symmetric, $a(-l) = -a(l-1)$ for $l = 1, 2, \cdots$ holds analytically.

III. DISPERSION PROPERTIES

The numerical dispersion for the time-domain wavelet-Galerkin methods based on D_2, D_3, and D_4 is investigated and compared to that of the standard FDTD, S-MRTD based on Battle–Lemarié wavelets [2] and some high-order finite-difference schemes [6]. Preliminary experiments showed that, for those wavelet-based schemes, the smaller stability factor s gives a smaller dispersion error as in S-MRTD, while for FDTD, the maximum stability limit gives the smallest dispersion error. In Figs. 1 and 2, the frequency deviation from the linear dispersion relation is plotted as a function of the normalized wavenumber $\chi = |\boldsymbol{k}|\Delta l$, where $\Delta l = \Delta x = \Delta z$ and $\boldsymbol{k}$ is the wave vector. The dispersion relation was obtained by substituting a time-harmonic trial solution into the update equations and numerically solving the resulting nonlinear equation [7]

$$\left(\frac{\Delta l}{c\Delta t}\right)^2 \sin^2\left(\frac{\Omega}{2}\right) = \left\{\sum_{l=0}^{L_s-1} a(l) \sin\left[\chi(\sin\theta)\left(l+\frac{1}{2}\right)\right]\right\}^2 + \left\{\sum_{l=0}^{L_s-1} a(l) \sin\left[\chi(\cos\theta)\left(l+\frac{1}{2}\right)\right]\right\}^2 \quad (7)$$

where c is the speed of light, $\Omega = \omega\Delta t$ the normalized frequency, and θ the angle of propagation.

Figs. 1 and 2 show that the dispersion error is largest for axial propagation and smallest for diagonal propagation. From these figures, it is found that a scaling function with a larger number of vanishing moments gives a smaller dispersion error. Note that, by virtue of the minimum support of Daubechies' compactly supported scaling functions, the connection coefficients

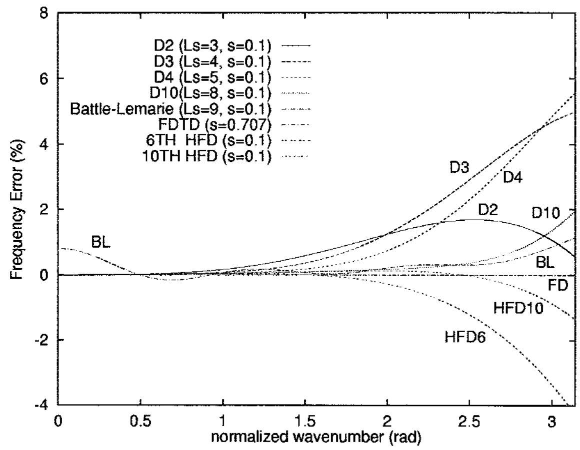

Fig. 1. Numerical dispersion relation for diagonal propagation at 45° with respect to the main axes. The stability factor is $s = 0.1$ for all the schemes except for FDTD where $s = 1.0/\sqrt{2}$. L_s denotes the stencil size or the number of connection coefficients in the update equations. HFD stands for high-order finite-difference scheme.

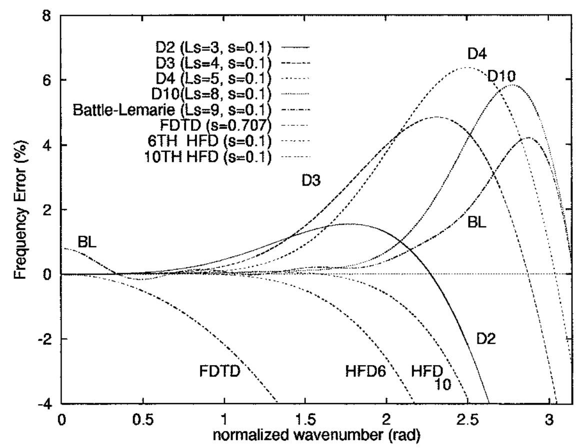

Fig. 2. Numerical dispersion relation for propagation along the main axes.

$a(l)$ concentrate on smaller l, resulting in a smaller number of coefficients in the update equations; for D_3, only the first four coefficients, and for D_4, only the first five coefficients give results with negligible errors, while for Battle–Lemarié scaling functions with $L_s = 9$, the dispersion relation does not converge as the wavenumber tends to zero.

IV. NUMERICAL RESULTS

Resonator structures depicted in Fig. 3 were analyzed with the wavelet-Galerkin method based on D_2, D_3, and D_4 scaling functions as well as with the standard FDTD method. The stability factor for D_2, D_3, and D_4 was chosen to be $s = 0.1$ while for FDTD, it was the maximum Courant limit $s = 1/\sqrt{2}$ to obtain the best accuracy. The length of the time-series was 100 for resonators a and b, and 1000 for resonator c. The perfect electric/magnetic conductor (PEC/PMC) conditions were implemented using the mirror principle. The results are shown in Table II. Although D_2, D_3, and D_4 are not symmetric, through the shifted interpolation property, it is possible to mirror the field coefficients with respect to the boundary to yield a symmetric boundary conditions only at integer points.

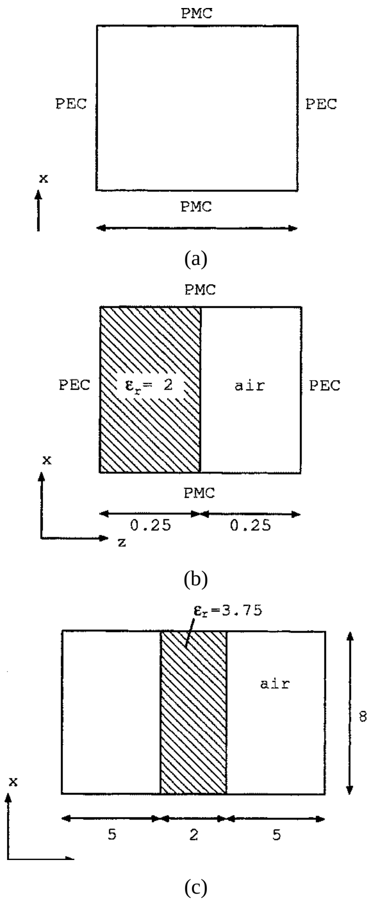

Fig. 3. (a) An air-filled infinitely large parallel plate resonator. (b) An infinitely large parallel plate resonator partially filled with a dielectric material. (c) A rectangular cavity with a centered dielectric slab.

TABLE II
DOMINANT RESONANT FREQUENCIES F_r, NUMBER OF TIME STEPS $N_{\max}$ AND CPU TIME FOR THE ANALYSIS OF THE RESONATORS. THE THEORETICAL RESONANT FREQUENCIES OF THE RESONATORS a, b, AND c ARE 1.0, 0.805 737, AND 0.052 21, RESPECTIVELY

Resonator	No. of Yee cells	Conditions	FDTD	$D_2\,(L_s = 3)$	$D_3\,(L_s = 4)$	$D_4\,(L_s = 5)$
a	10×10	N_{max}	2828	20000	20000	20000
		F_r	0.99793	1.000076	0.999979	0.999959
		error (%)	-0.207	+0.0076	-0.0021	-0.0041
		CPU time (s)	0.5	3.2	3.6	4.2
	4×4	N_{max}	—	8000	8000	8000
		F_r	—	1.00203	1.00077	1.00030
		error (%)	—	+0.203	+0.077	+0.03
		CPU time (s)	—	1.0	1.0	1.1
b	10×10	N_{max}	4000	28285	28285	28285
		F_r	0.80322	0.80644	0.80633	0.80633
		error (%)	-0.31	+0.087	+0.073	+0.073
		CPU time (s)	0.6	4.0	4.7	5.5
	4×4	N_{max}	—	11314	11314	11314
		F_r	—	0.8109	0.8100	0.8095
		error (%)	—	+0.64	+0.53	+0.47
		CPU time (s)	—	0.8	0.9	1.0
c	8×12	N_{max}	2738	19364	19364	19364
		F_r	0.05232	0.05272	0.05271	0.05271
		error (%)	+0.21	+0.98	+0.96	+0.96
		CPU time (s)	0.5	3.3	3.6	4.2
	2×12	N_{max}	—	14144	14144	14144
		F_r	—	0.05316	0.05329	0.05307
		error (%)	—	+1.88	+2.07	+1.65
		CPU time (s)	—	1.3	1.5	1.8

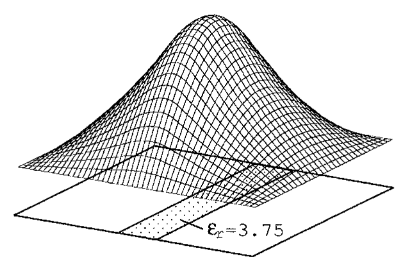

Fig. 4. E_y distribution of the resonator c in Fig. 3. The structure is discretized with 8×12 Yee cells and the field is sampled with 4×4 times higher density.

For axial propagation in a homogeneous medium (resonator a), D_2, D_3, and D_4 give much more accurate results than FDTD. These results are consistent with the dispersion relation shown in Fig. 2. With inhomogeneous dielectric media (resonator b), those scaling functions still give better results than FDTD, but the accuracy degrades compared to the homogeneous case.

For the cavity resonator with a centered dielectric slab, the standard FDTD is more accurate than the wavelet-Galerkin method; this is expected from the dispersion relation (Fig. 1) because, for this resonant mode, the diagonal propagation is dominant over the axial propagation and FDTD has much less numerical dispersion than the wavelet-Galerkin method. It was also found that, for the given examples, D_4 gives better accuracy than D_2. Another advantage of D_4 over D_2 is that reconstructed field distributions are smoother; see, in Fig. 4, the E_y distribution of resonator c where the structure is discretized with 8×12 Yee cells and the field is sampled with 4×4 times higher density.

The wavelet-Galerkin method requires more CPU time than FDTD with the same number of grids mainly because the time step Δt is approximately seven times smaller. However, for electrically large three-dimensional structures where FDTD is computationally too expensive to use, reduction of CPU time and memory requirement compared to FDTD is expected.

V. CONCLUSION

The time-domain wavelet-Galerkin method based on Daubechies' compactly supported scaling functions with two, three, and four vanishing moments has been investigated. The minimum support property of Daubechies' scaling functions results in a smaller number of stencil size than is expected from the theoretical support size. It was found that the shifted interpolation property is applicable to D_3 and D_4, and that, in particular for the axial propagation in an homogeneous medium, D_4 gives much higher accuracy than D_2 and FDTD.

REFERENCES

[1] Y. W. Cheong, Y. M. Lee, K. H. Ra, J. G. Kang, and C. C. Shin, "Wavelet-Galerkin scheme of time-dependent inhomogeneous electromagnetic problems," *IEEE Microwave Guided Wave Lett.*, vol. 9, pp. 297–299, Aug. 1999.

[2] M. Krumpholz and L. P. B. Katehi, "MRTD: New time-domain schemes based on multiresolution analysis," *IEEE Trans. Microwave Theory Tech.*, vol. 44, pp. 555–571, Apr. 1996.

[3] K. S. Yee, "Numerical solution of initial boundary value problems involving Maxwell's equation in isotropic media," *IEEE Trans. Antennas Propagat.*, vol. 14, pp. 302–307, May 1966.

[4] I. Daubechies, *Ten Lectures on Wavelets*. Philadelphia, PA: SIAM, 1992.

[5] W. Sweldens and R. Piessens, "Wavelet sampling techniques," in *Proc. Statistical Computing Section*, 1993, pp. 20–29.

[6] W. Y. Tam, "Comments on "new prospects for time domain analysis"," *IEEE Microwave Guided Wave Lett.*, vol. 6, p. 422, Nov. 1996.

[7] A. Taflove, *Computational Electrodynamics—The Finite-Difference Time-Domain Method*. Norwood, MA: Artech House, 1995.